Supplemental Materials

Molecular Biology of the Cell

Zaytsev et al.

Multisite phosphorylation of the NDC80 complex gradually tunes its microtubule-binding affinity

Anatoly V. Zaytsev[1], Jeanne E. Mick[2], Evgeny Maslennikov[3], Boris Nikashin[1],

Jennifer G. DeLuca[2,*] and Ekaterina L. Grishchuk[1,*]

[1]Physiology Department, Perelman School of Medicine, University of Pennsylvania, Philadelphia, PA, USA 19104

[2]Department of Biochemistry and Molecular Biology, Colorado State University, Fort Collins, CO, USA 80523

[3]Center for Theoretical Problems of Physico-chemical Pharmacology, RAS, Moscow, Russia 119991

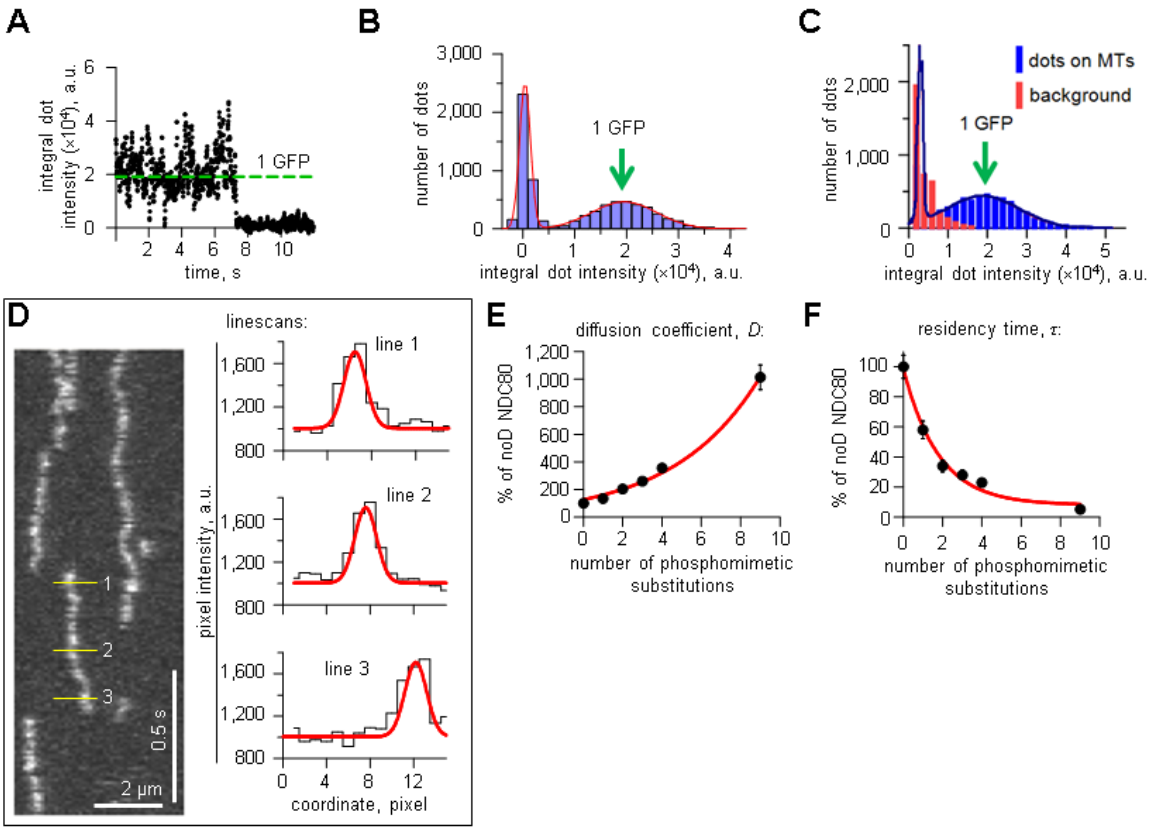

Figure S1

Figure S1. Quantitative analysis of single NDC80 complex fluorescence, binding and diffusion on the MT

(A) Typical photobleaching curve for an NDC80-GFP complex adsorbed non-specifically to the coverslip (exposure time 10 ms). Background intensity was subtracted. Position of green line corresponds to the brightness of a single GFP, as determined from the histogram in panel B. (B) Histogram of integrated dot intensities for coverslip-adsorbed NDC80 complexes (data for 10 photobleaching dots, generating 7,471 intensity measurements). Fitting is the sum of two Gaussian distributions; mean intensity for the second peak (green arrow) shows that the brightness of a single GFP molecule in these experiments was (1.95 ± 0.03) × 10^4 a.u. (C) Histogram of integrated dot intensities for the MT-associated noD NDC80 complexes (number of measurements 8,296). Fitting is the sum of two Gaussian distributions. The distance between two peaks is (1.87 ± 0.04) × 10^4 a.u., which corresponds well to the intensity of a single GFP determined using coverslip-adsorbed NDC80 molecules (D) Example of semi-automated analysis of the diffusion tracks using kymographs of single NDC80 complexes. Yellow horizontal lines indicate positions of the example linescans across one track, see graphs on the right. The linescans were fitted with Gaussians (red curves) to determine dot position vs. time; peak position of the Gaussian was used as a

dot positon. (E) Diffusion coefficients for different phosphomimetic NDC80 mutants. Diffusion coefficient for noD NDC80 was taken as 100%; red curve is exponential fit (R^2 = 0.9953). (F) Analogous to panel E graph but for residency time; red line is exponential fit (R^2 = 0.9879).

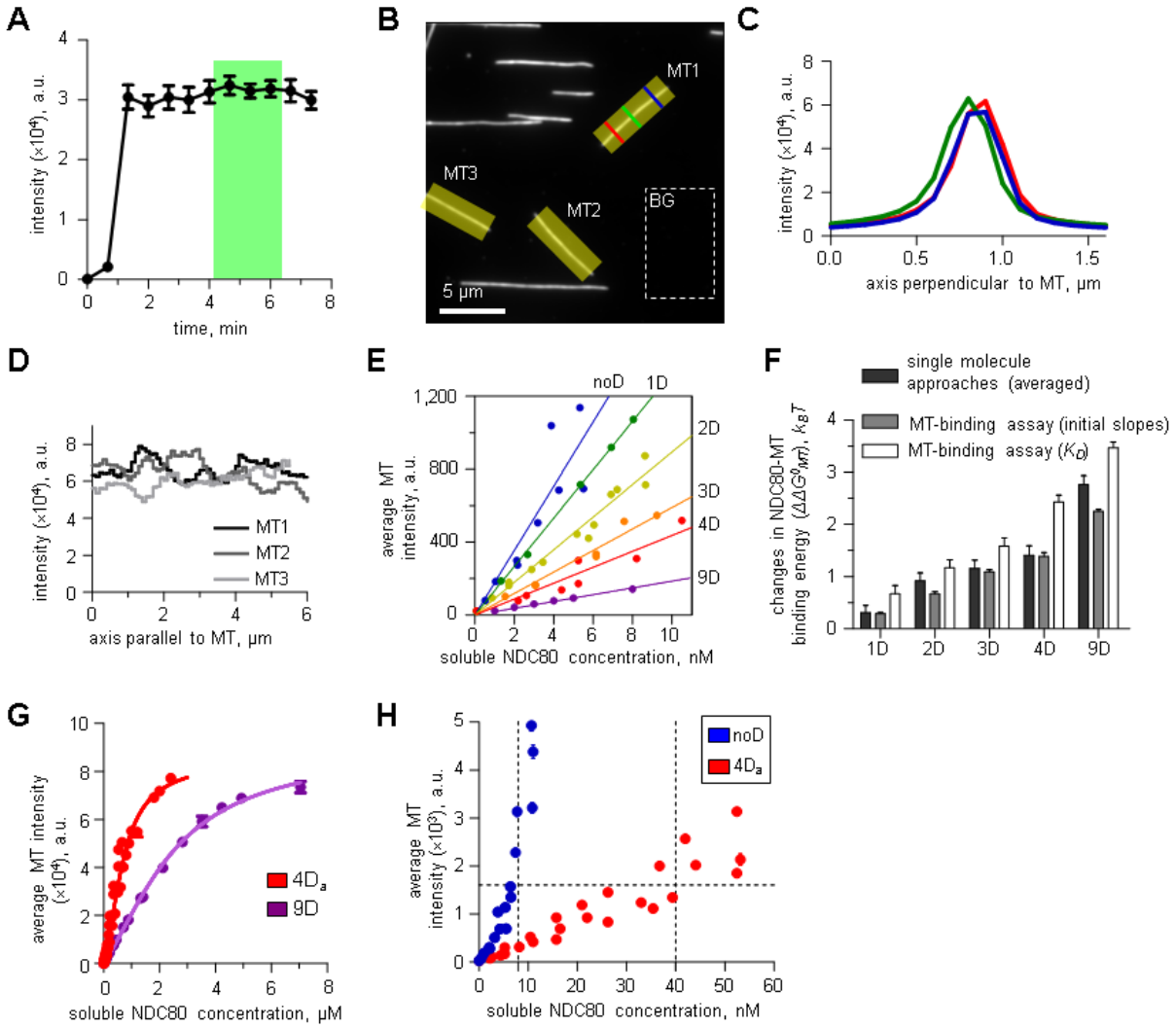

Figure S2

Figure S2. TIRF-based MT-binding assay

(A) Kinetics of changes in MT decoration intensity in a flow chamber after the start of NDC80-GFP protein perfusion (time 0) with a peristaltic pump. Data shown are for noD NDC80 complex (40 nM). Intensity increases after 1 min and then remains constant. To ensure reproducibility of our quantitative

experiments, images were acquired 4 min after the start of perfusion for approximately 2 min (time interval shown in green). (B) Typical image of a field of MTs decorated with NDC80-GFP (noD, 280 nM). MTs were selected with rectangular regions (yellow boxes for 3 representative MTs). For each line across such a region, the intensity profile was recorded (see panel C). Background level was defined as the average intensity of the image area without MTs (BG, dotted rectangle). In this example BG = 990 a.u. (C) Examples of the MT intensity profiles for three linescans perpendicular to MT1 (colored lines on panel B). (D) Peak intensities along three representative MTs in panel B. Intensity values on this graph are the peak intensities of the linescans that were taken perpendicularly to the MT axis (shown in panel C). (E) Initial segments for the MT-binding curves (Figure 5B) at low NDC80 concentrations. The slope of the initial segment provides an independent measure of the relative energy of MT binding of single NDC80 molecules. (F) Changes in NDC80-MT binding energy in response to the increasing number of phosphomimetic substitution relative to the noD NDC80 protein. These values were determined from the single molecule measurements (average of two approaches in Figure 4D), the initial slopes (panel E) and the K_D values, which were determined by applying a wide range of NDC80 concentrations (Figure 5B). Error bars are SEM. (G) MT-binding curves for the $4D_a$ and 9D NDC80 mutants for 0 – 8 μM protein concentration (same data as in Figure 5B but plotted for 0 - 0.8 μM range). Symbols are average data for two independent experiments; errors are SEM. Solid lines are the fits with the model schematized in Figure 5C. (H) MT-binding data for noD and $4D_a$ NDC80 complexes for 0 – 60 nM protein concentration. For our FRAP experiments at low MT decoration density, the concentrations of noD and $4D_a$ NDC80 complexes were chosen as 8 nM and 40 nM (vertical dashed lines), respectively; these concentrations produced similar MT-decoration intensity (horizontal line).

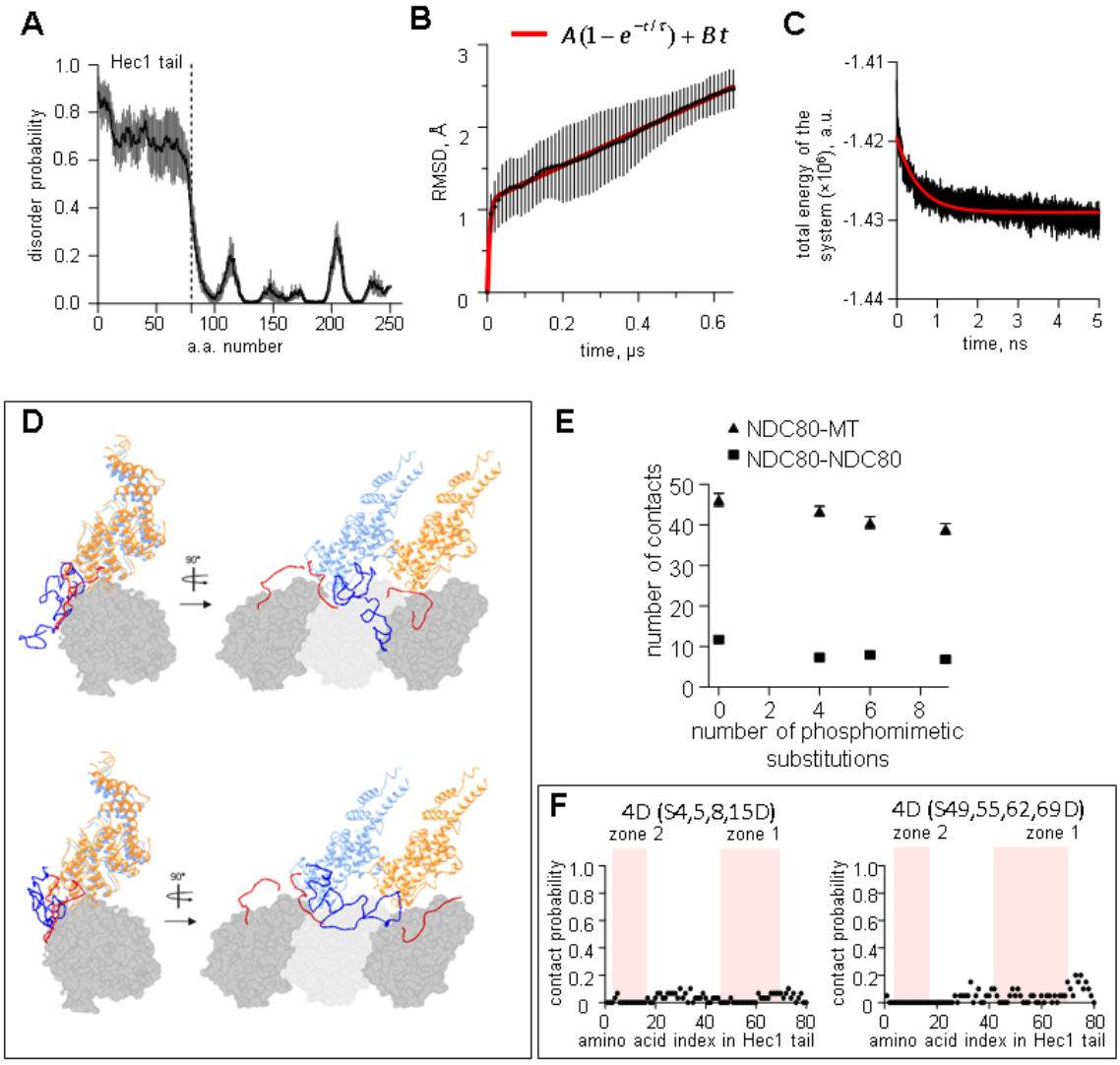

Figure S3

Figure S3. MD simulation analysis of the Hec1 tail conformation

(A) Disorder probability of the first 250 a.a. of Hec1 was obtained using four web-based resources and the outputs were averaged (black line); SEM intervals are shown in grey. (B) Changes in RMSD during MD simulation of the Hec1 tail in solution (start at time zero). Bars are SEM. (C) Total energy of the system plotted vs. time for one representative simulation that started with the compact Hec1 tail, as in Figure 7D. Red curve is exponential fit. (D) Two example structures obtained after the MD simulations of the NDC80-MT patch with the Hec1 tail initially configured in a fully extended conformation. (E) Number of contacts between one MT-bound NDC80 complex and the MT (triangles) or between two adjacent NDC80 complexes (squares); n ≥ 16 simulations were carried out for each protein with the indicated

number of phosphomimetic substitutions in the Hec1 tail. For NDC80 with 4 substitutions the average value for two tails (with phosphomimetic substitutions located in “zone 1” or “zone 2”) is plotted. (F) Black dots show calculated contact probability between different a.a. in the Hec1 tail with indicated substitutions and a neighboring NDC80 complex. Pink areas highlight zone 1 and zone 2 in the Hec1 tail. Data are based on $n \geq 20$ simulations with an initially unfolded Hec1 tail.